Vapor–Liquid Equilibria of Water–Hydrogen Chloride Solutions below 0 °C

Eugene Miller

Chemical and Metallurgical Engineering Department, Mackay School of Mines, University of Nevada—Reno, Reno, Nevada 89557

The vapor–liquid equilibria of 4–36 wt % (0.0411–0.2145 mole fraction) HCl–water solutions were determined for temperatures between 0 and −40 °C. Total pressures were measured by capacitance gauges, vapor compositions by direct vapor-phase sampling into a quadrupole mass filter, and liquid compositions by electric conductivity. Vapor compositions were also predicted thermodynamically from the total pressure and liquid composition data by means of the Gibbs–Duhem equation.

Introduction

Water–hydrogen chloride solutions exhibit a maximum boiling temperature azeotrope at low pressure and a liquid-phase separation at high pressure. Perry's handbook (*1*) contains a compilation of the partial pressures of water and HCl over aqueous HCl solutions from 2 to 46 wt % HCl for 0–110 °C based on Zeisberg's (*2*) compilation of low-pressure data. Fritz and Fuget (*3*) and Othmer and Naphtali (*4*) calculated the vapor–liquid equilibria from the emf data of Harned and Ehlers (*5*, *6*) and Akerlof and Teare (*7*) from 0 to 50 °C and for 0.01–15.8 *m* HCl solutions. The calculated partial pressures of HCl for 6–11 *m* solutions agreed within 5% of those compiled by Zeisberg from manometric and calorimetric data. Experimental difficulties at concentrations lower than 0.6 *m* gave less consistent results and the computations from the emf measurements were more reliable. Rupert (*8*) and later Thumm et al. (*9*) measured the solubility of HCl in water at high pressures and higher molalities. More recently, Kao (*10*) determined the vapor–liquid equilibria at intermediate molalities and pressures.

There are no published vapor–liquid equilibria data for liquid solutions containing 36 wt % HCl or less at temperatures below 0 °C possibly because of experimental difficulties. The present experimental study was designed to fill this need for temperatures nominally between 0 and −40 °C for 4–36 wt % HCl solutions (0.0411–0.2145 mole fraction HCl).

Experimental Section

The experimental method chosen was an adaptation of one described by Dunn and Rideal (*11*), distilling a small quantity of HCl and water from a relatively large volume of solution. The solutions used were made up from ACS reagent-grade 12 N hydrochloric acid with no further purification and diluted as required with laboratory-distilled water. As shown schematically in Figure 1, a 2-L Pyrex flask containing the test solution was immersed in an insulated methylene chloride bath cooled by a two-stage mechanical refrigeration system. The temperature of the bath was maintained within ±0.1 °C monitored by a calibrated platinum resistance thermometer. The thermometer was calibrated at the ice point and the sublimation temperature of solid carbon dioxide at 1 atm. Removal of air from the system was effected by a mechanical vacuum pump in series with a liquid-nitrogen trap. Equilibrium pressures were measured with two MKS Baratron type 220 capacitance gauges (1×10^{-4}–1 torr and 1×10^{-2}–1×10^{2} torr) calibrated by the manufacturer using a transfer standard calibrated with a CEC air dead-weight tester to ±0.02% of full scale accuracy. Samples of the liquid were analyzed by electroconductivity measurements at 25 ± 0.1 °C using a Barnstead Model PM-70CB bridge and a Yellowstone Springs YSI 3400 Pyrex cell with a maximum deviation of ±1%. Samples of the vapor were drawn directly from the vapor chamber into a Varian VGA-100 quadrupole mass filter where the mole fractions were derived from the recorded mass-spectral areas in the range 34–39 and 15–20 mass numbers for HCl and water, respectively. The spectra were obtained at a pressure of nominally 3.0×10^{-6} torr, sampling continuously from the vapor chamber into the quadrupole mass filter pumped by a Varian 20 L/s Vacion pump. Since the total pressures in the vapor chamber were sufficiently low, the partial pressures of the HCl and water were calculated from the ideal gas law.

All valves, tubing, and fittings were made of AISI 304 or 315 stainless steel. Viton O-rings and copper gaskets were used in the valves and flanges, respectively. All metal parts in continuous contact with the vapor were coated with silicone vacuum grease. No significant corrosion of any of the metals was observed so long as care was taken to avoid contact with liquid acid.

The experimental procedure followed was as follows:

(1) The solution was allowed to equilibrate to the selected temperature for at least 18 h. The whole system was then evacuated to a pressure below the range of the gauges. The solution itself was deaerated by slowly opening the flask to the evacuated vapor chamber, allowing the system pressure to rise to the vapor pressure of the solution, shutting off the flask, and reevacuating the vapor chamber, etc., 5 times.

(2) After deaeration, the flask valve was opened slowly, admitting vapor to the vapor chamber and measuring the total pressure as a function of time over a minimum of 16 min. Measurements were repeated generally 5 times with five deaeration cycles between runs. Small corrections to the measured pressure for minor leaks and adsorbed gases in the vapor chamber were derived from the slope of the vapor pressure curve once equilibrium had been achieved.

(3) Subsequently, mass-spectrographic analyses were made by bleeding gases continuously into the gas analyzer over a 2-h period, permitting the analyzer system to come to equilibrium. The gas analyzer was pumped to 1×10^{-8} torr prior to admitting the gas sample. Corrections were made for background water and HCl present in the gas analyzer.

(4) Liquid samples were taken from the flask after each sequence of pressure and spectral measurements. The samples were subsequently diluted with distilled water by 50:1 to 150:1 depending on the sample's acid concentration. The diluted sample conductivities were then measured and compared with certified N/30 and N/10 hydrochloric acid reagent standards. Only small differences in acid concentrations were detected from sample to sample for a given solution, well within the precision of the analyses.

Quadrupole Mass Filter Relative Sensitivity to Water and HCl. The quadrupole mass filter does not exhibit the same sensitivity to HCl and water vapor. It was therefore necessary to establish the relative sensitivities. Pure HCl and water vapor were introduced separately into the mass filter over a range of

0021-9568/83/1728-0363$01.50/0

Table I. Comparison of Experimental Results with Predicted and Literature Values at 0 °C[a]

	total press.			partial press. of HCl				partial press. of H_2O			
x_{HCl}	exptl	FF	PH	exptl	GD	FF	PH	exptl	GD	FF	PH
0.0411	4.19	4.12	4.01		7.1×10^{-5}	3.0×10^{-4}	1.64×10^{-4}	(4.14)	4.19	4.12	4.01
0.0723	3.56	3.58	3.43		1.3×10^{-5}	2.31×10^{-5}	2.06×10^{-5}	(3.47)	3.56	3.58	3.43
0.1150	2.57	2.73	2.55	0.039	0.037	0.047	0.045	2.51	2.53	2.68	2.50
0.1545	2.30	2.42	2.27	0.76	0.69	0.63	0.64	1.54	1.61	1.79	1.63
0.1896	7.02	6.19	7.03	6.07	5.97	5.05	6.00	0.95	1.05	1.14	1.03
0.2145	28.20	20.91	25.22	(26.45)	27.51	20.10	24.50		0.69	0.805	0.72

[a] Exptl, experimental results; FF, Fritz and Fuget, ref 3; PH, Perry's handbook, ref 1; GD, Gibbs-Duhem equation predicted results. Pressures are in torr.

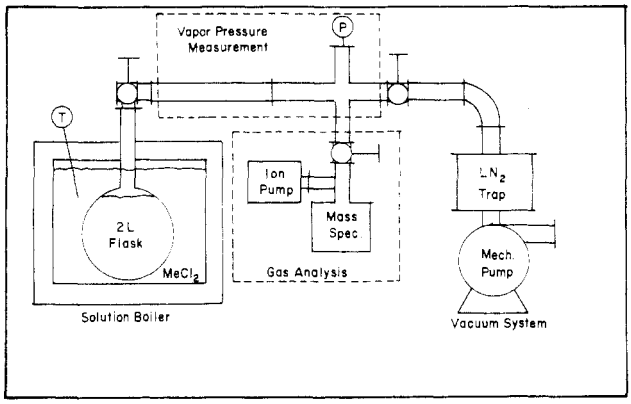

Figure 1. Schematic of experimental apparatus.

instrument pressures of 0.2×10^{-7}–3.0×10^{-6} torr. Measurements of spectral areas were made at a detector sensitivity of 1×10^{-10} and 1×10^{-9} amp/div with a 3-s sweep of the mass number ranges of 34–39 and 15–20 at a recorder setting of 0.5 V full-range and a chart speed of 1 in./s. The data for the HCl and water were each correlated by a least-squares fit of the spectral area and pressure. By comparing the spectral areas of HCl and water at the same pressure, we obtained the relative sensitivity of the instrument. The relative sensitivity of water to HCl was found to range from a limiting value of 3.79 at less than 1×10^{-8} torr to a maximum of 4.50 at 6.0×10^{-7} torr to 4.10 at 3.0×10^{-6} torr.

Results and Discussion

At the lowest liquid-solution HCl mole fractions studied, 0.0411 and 0.0723, the vapor compositions are predominantly water, and at the highest mole fraction of 0.2145, HCl. For these solutions, small errors in measurement of the dominant species led to large errors in the minor species. For these cases, the P and x_{HCl} data which are reliable were used in conjunction with the Gibbs–Duhem equation to compute the vapor compositions and subsequently the equilibrium partial pressures of these solutions. The computations were used additionally to establish the consistency of all the vapor composition measurements at all liquid mole fractions and temperatures.

For the low pressures of these experiments, the Gibbs–Duhem equation may be written

$$dy/dP = [1 - PV^*/RT]y(1 - y)/P(y - x) \quad (1)$$

Integration of eq 1 provides the desired relation between P, y_{HCl}, and x_{HCl} based on the input of P–x_{HCl} data. Since at the azeotrope, the vapor and liquid mole fractions are equal and eq 1 is indeterminate, a relation for the starting value of dy/dx at the azeotrope is required. From Van Ness (12)

$$(dy/dx)_{az} = \frac{1}{2} \pm (\frac{1}{4} - m)^{1/2} \quad (2)$$

where

$$-m = \{d^2P/dx^2\}_{az}[y_{az}(1 - y_{az})/P_{az}] \quad (2a)$$

The value of y_{az} was obtained by interpolation from smoothed experimental P–x_{HCl} data. A polynomial equation in P and x_{HCl} was derived from a least-squares fit permitting computation of $(d^2P/dx^2)_{az}$. m and the starting value of $(dy/dx)_{az}$ were derived from eq 2 and 2a. Equation 1 then was integrated by a numerical marching procedure starting at the azeotrope. The term PV^*/RT was found to be negligible for the experimental conditions.

Comparison of Experimental and Literature Data at 0 °C. In Table I, a summary is given of the smoothed experimental data, the partial pressures, and vapor compositions computed from the Gibbs–Duhem equation, and the literature data from ref 1, 3, and 4 at 0 °C. Fritz and Fuget (3) and Othmer and Naphtali (4) concluded that the vapor pressures predicted from the precise measurements of cell potential were probably more nearly correct than the direct vapor pressure measurements given in ref 1, particularly for low vapor pressure ranges. Their conclusions are not completely supported by the present experimental measurements. At the lowest x_{HCl} values, 0.0411 and 0.0723, the experimental values for total pressure indeed agree better with their calculations, but at all other more concentrated liquid solutions, the Perry's handbook (1) data are closer. Deviations of the present experimental data from the values predicted from cell data are 0.6–1.7% at the lower x_{HCl} values, and 0.1–1.3% from the Perry's handbook data at higher x_{HCl} values of 0.1150–0.1896. At the highest mole fraction of HCl of 0.2145, the handbook data are closer to the experimental results but are 11.8% low.

For x_{HCl} of 0.1150–0.2145, the predicted Gibbs–Duhem p_{HCl} values agree with experiment to within 1.7–10.1%. The Perry's handbook data agree better with these experiments than the cell data with a deviation of 1.2–18.8%. At the lowest liquid-solution mole fractions of 0.0411 and 0.0723, the Gibbs–Duhem predictions for p_{HCl} are 60–180% lower than either set of literature data. Based on the overall consistency of the Gibbs–Duhem prediction, the results are believed to be correct to 10% or better.

For x_{HCl} values of 0.0411–0.1896, the Gibbs–Duhem predicted p_{H_2O} values agree with experiment to within 0.8–10.5%. At x_{HCl} of 0.0411–0.0723, both the cell and vapor pressure literature values agree with the experimental data to 1–3%. At the higher x_{HCl} values, Perry's handbook agrees better with experimental data, 0.4–8.4%. In addition, at an x_{HCl} of 0.2145 the Perry's handbook data match the Gibbs–Duhem predictions better than the cell data, 4.3%.

Experimental Data and Predicted Values. The unsmoothed experimental data are displayed in Figures 2–4. In these figures, total equilibrium pressure, P, partial pressure of water, p_{H_2O}, and the partial pressure of HCl, p_{HCl}, are plotted as a function of solution temperature, T, at constant liquid mole fraction of HCl, x_{HCl}. Data from Perry's handbook (1) are shown for comparison. A summary of all the smoothed experimental results and the computed Gibbs–Duhem partial pressures and vapor compositions is given in Table II. Average, standard, and maximum deviations of the experimental total pressure, vapor compositions, and partial pressures from

Table II. Vapor-Liquid Equilibria of HCl-Water Solutions

			exptl				Gibbs-Duhem prediction			
x_{HCl}	T, °C	P, torr	y_{HCl}	y_{H_2O}	p_{HCl}, torr	p_{H_2O}, torr	y_{HCl}	y_{H_2O}	p_{HCl}, torr	p_{H_2O}, torr
0.0411	0	4.19		(0.987)		(4.14)	1.7×10^{-5}	1.000	7.1×10^{-5}	4.19
	−10	2.00		(0.990)		(1.98)	8.1×10^{-6}	1.000	1.6×10^{-5}	2.00
0.0723	0	3.56		(0.974)		(3.47)	3.8×10^{-4}	1.000	1.3×10^{-3}	3.56
	−10	1.61		(0.990)		(1.59)	3.5×10^{-4}	1.000	5.7×10^{-4}	1.61
0.1150	0	2.57	0.015	0.985	0.039	2.51	0.014	0.986	0.037	2.53
	−10	1.18	0.016	0.984	0.019	1.16	0.014	0.986	0.016	1.16
	−20	0.475	0.020	0.980	0.0095	0.466	0.014	0.986	0.0066	0.468
	−30	0.187	0.024	0.976	0.0044	0.183	0.012	0.988	0.0022	0.185
	−35	0.119	0.027	0.973	0.0032	0.116				
0.1545	0	2.30	0.329	0.671	0.76	1.54	0.302	0.698	0.69	1.61
	−10	1.02	0.238	0.762	0.24	0.78	0.265	0.735	0.27	0.75
	−20	0.407	0.170	0.830	0.069	0.338	0.123	0.877	0.050	0.357
	−30	0.152	0.129	0.871	0.020	0.132	0.121	0.879	0.018	0.134
	−35	0.094	0.117	0.883	0.011	0.083				
0.1896	0	7.02	0.865	0.135	6.07	0.95	0.851	0.149	5.97	1.05
	−10	3.12	0.858	0.142	2.68	0.44	0.849	0.151	2.65	0.47
	−20	1.28	0.828	0.172	1.06	0.22	0.854	0.146	1.09	0.19
	−30	0.499	(0.727)		(0.363)		0.862	0.138	0.430	0.069
0.2145	0	28.20			(26.45)		0.976	0.024	27.51	0.69
	−10	15.90			(14.79)		0.981	0.019	15.59	0.31
	−20	7.41			(6.84)		0.985	0.015	7.30	0.11
	−30	2.88			(2.64)		0.985	0.015	2.84	0.043

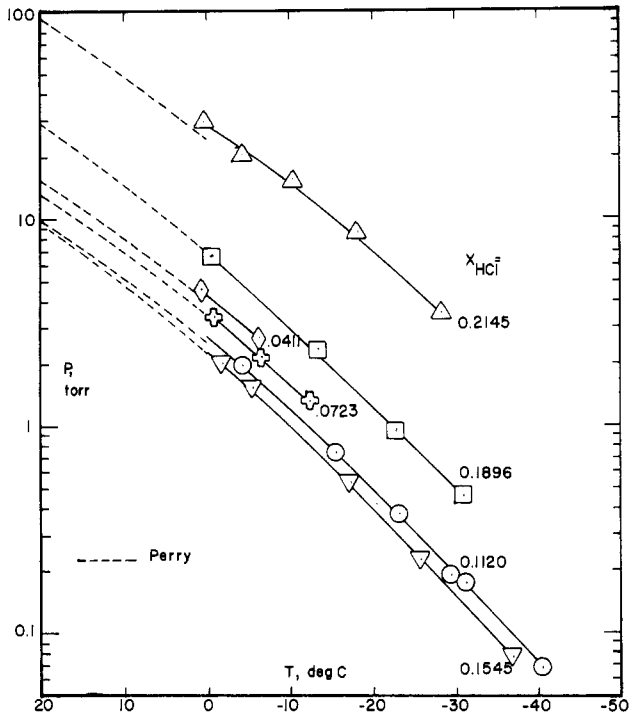

Figure 2. Total vapor pressure, P, as a function of mole fraction of HCl, x_{HCl}, and temperature, T.

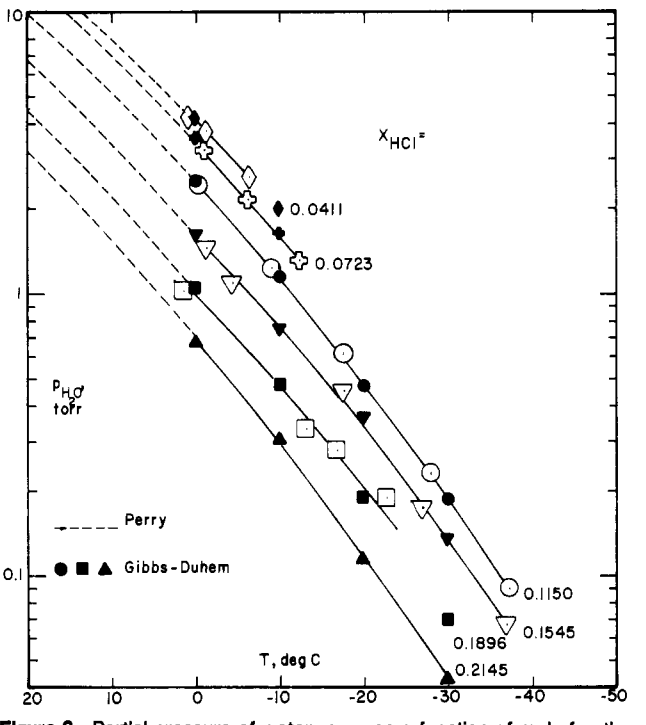

Figure 3. Partial pressure of water, p_{H_2O}, as a function of mole fraction of HCl, x_{HCl}, and temperature, T.

their respective smoothed values are given in Table III. As shown in Table III, the standard deviation of the experimental total pressure data in Figure 2 is 5.8% for an x_{HCl} of 0.2145. In general, scatter increased with increasing hydrogen chloride concentration in the liquid phase. The maximum deviation observed was 8.9% and was independent of liquid composition. At lower values of x_{HCl}, as the vapor becomes progressively higher in water content the standard deviation of y_{H_2O} decreases. The opposite behavior is seen in the scatter of the y_{HCl} values. A similar variation in deviation of experimental and smoothed partial pressures is seen also. The observed variation in standard and maximum deviations is a reflection of the greater sensitivity of the quadrupole mass filter to water than to hydrogen chloride.

Since at an x_{HCl} of 0.2145 and below an x_{HCl} of 0.1150 the quadrupole mass filter is incapable of accurate analysis, only the Gibbs–Duhem predicted p_{HCl} and p_{H_2O} values are shown in Figures 3 and 4 for these conditions. The relations of experimental, predicted, and Perry's handbook values with x_{HCl} and temperature are consistent. In Figure 4, the correlation of the Gibbs–Duhem predicted p_{HCl} values with temperature at x_{HCl} values of 0.0723 and 0.0411 is much lower than would be obtained by an extrapolation of the literature data above 0 °C, as discussed previously.

A typical Gibbs–Duhem prediction of y_{HCl} vs. x_{HCl} for a solution temperature of −10 °C is plotted in Figure 5. The experimental y_{HCl} data at all temperatures are higher than predicted for x_{HCl} below 0.1 and lower for x_{HCl} greater than 0.2. At 0 °C, the Perry's handbook y_{HCl} data are closer to the

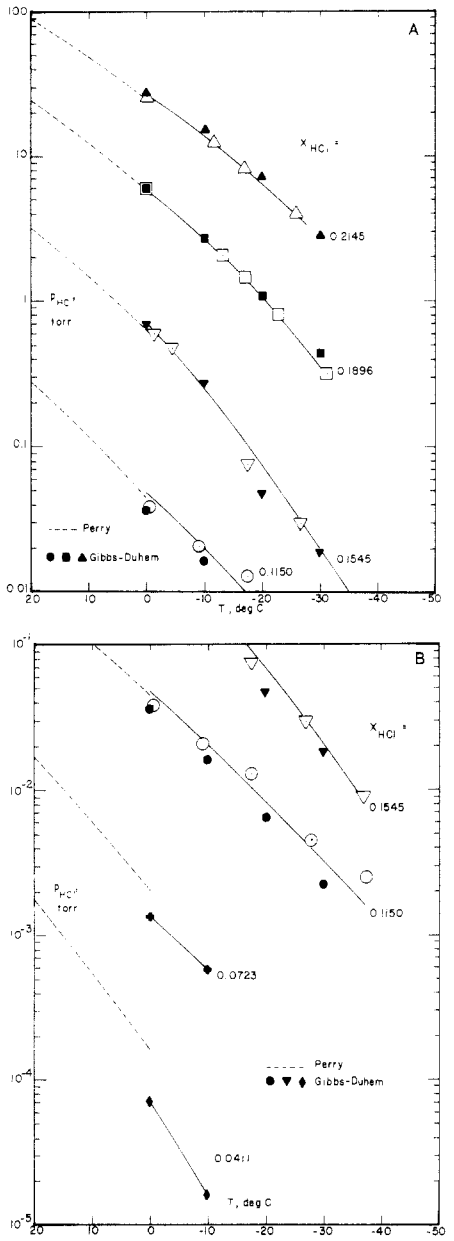

Figure 4. Partial pressure of HCl, p_{HCl}, as a function of mole fraction of HCl, x_{HCl}, and temperature, T.

predicted values for these extreme x_{HCl} values than the present experimental data. Those partial pressure results that are relatively inaccurate compared with other data and the predicted values are so indicated by parentheses in Tables II and III. For these cases, the Gibbs–Duhem predicted values are recommended.

Glossary

p_{HCl}	partial pressure of hydrogen chloride
p_{H_2O}	partial pressure of water
P	total pressure
R	gas constant
T	temperature
V^*	excess molar volume
x	liquid-phase mole fraction
x_{HCl}	liquid-phase mole fraction of hydrogen chloride
y	gas-phase mole fraction
y_{HCl}	gas-phase mole fraction of hydrogen chloride

Table III. Percentage Deviation of Experimental from Smoothed Data[a]

	total press.		
x_{HCl}	AD	SD	MD
0.0411	0	0	0
0.0723	0	0	0
0.1120	0.3	0.7	−8.9
0.1545	0	0	0
0.1896	0.5	0.7	+5.8
0.2145	4.2	5.8	−8.3

	vapor composition					
	y_{H_2O}			y_{HCl}		
x_{HCl}	AD	SD	MD	AD	SD	MD
0.0411						
0.0723						
0.1150	0.1	0.2	+0.4	4.7	9.4	−20.5
0.1545	2.3	1.8	+5.0	8.5	6.6	−28.6
0.1896	1.4	1.9	−5.8	0.3	0.5	+0.9
0.2145						

	partial press.					
	p_{H_2O}			p_{HCl}		
x_{HCl}	AD	SD	MD	AD	SD	MD
0.0411						
0.0723						
0.1150	1.7	1.8	+4.0	20.2	26.2	−41.2
0.1545	3.6	4.1	+8.4	6.0	9.3	−21.1
0.1896	14.3	17.0	+20.3	3.3	3.3	−16.7
0.2145						

[a] AD, average deviation; SD, standard deviation; MD, maximum deviation.

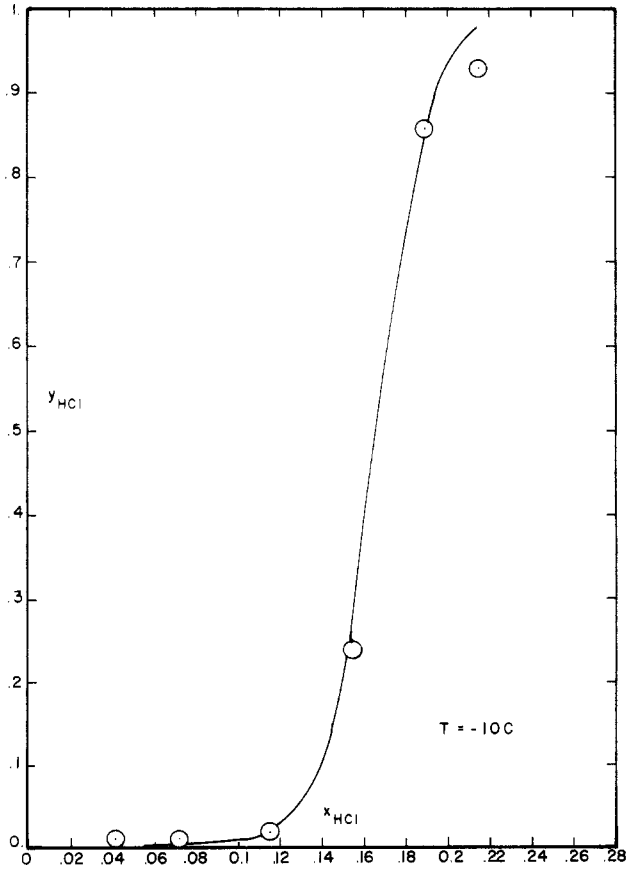

Figure 5. Gibbs–Duhem prediction of y_{HCl} vs. x_{HCl} for T = −10 °C.

y_{H_2O} gas-phase mole fraction of water

Registry No. HCl, 7647-01-0.

Literature Cited

(1) Perry, J. H. "Chemical Engineer's Handbook", 3rd ed.; McGraw-Hill: New York, 1950; p 166.
(2) Zelsberg, F. C. *Chem. Metall. Eng.* **1925**, *32*, 326.
(3) Fritz, J. J.; Fuget, C. R. *Ind. Eng. Chem., Chem. Eng. Ser.* **1959**, *1*, 10.
(4) Othmer, D. F.; Naphtali, L. M. *Ind. Eng. Chem., Chem. Eng. Ser.* **1959**, *1*, 1.
(5) Harned, H. S.; Ehlers, R. W. *J. Am. Chem. Soc.* **1932**, *54*, 1350.
(6) Harned, H. S.; Ehlers, R. W. *J. Am. Chem. Soc.* **1933**, *55*, 2179.
(7) Akerlof, G.; Teare, J. W. *J. Am. Chem. Soc.* **1937**, *59*, 1855.
(8) Rupert, F. F. *J. Am. Chem. Soc.* **1909**, *31*, 851.
(9) Haase, R.; Naas, H.; Thumm, H. *Z. Phys. Chem. (Frankfurt am Main)* **1963**, *37*, 210.
(10) Kao, J. T. F. *J. Chem. Eng. Data* **1970**, *15*, 362.
(11) Dunn, J. S.; Rideal, E. K. *J. Chem. Soc.* **1924**, *125*, 676.
(12) Van Ness, H. C. *AIChE J.* **1970**, *16*, 18.

Received for review May 24, 1982. Revised manuscript received April 11, 1983. Accepted April 29, 1983. This work was supported by the U.S. Air Force Office of Scientific Research under Grant AFOSR-77-3333.

Measurements of Densities and Dielectric Constants of Liquid Isobutane from 120 to 300 K at Pressures to 35 MPa

William M. Haynes

Thermophysical Properties Division, National Engineering Laboratory, National Bureau of Standards, Boulder, Colorado 80303

Measurements of the densities and dielectric constants of compressed liquid isobutane have been carried out at temperatures between 120 and 300 K to pressures of 35 MPa. These experimental data along with computed values for the Clausius–Mossotti function (CM) are reported in this paper.

Introduction

This work is part of a large-scale program at this laboratory to determine the thermophysical properties of technically important fluids. In addition to isobutane being a major component of petroleum and natural gases, it is a prime candidate as a working fluid in geothermal energy processes. This work was undertaken to provide density and dielectric constant data for isobutane in regions not previously investigated.

Experimental Section

Detailed descriptions of the experimental apparatus and procedures have been presented in other papers (*1–5*). Only information essential to understand this paper is presented here.

Simultaneous measurements of density and dielectric constant were made on the same liquid samples. A magnetic suspension densimeter was used to obtain the density data, while a concentric cylindrical capacitor contained in the same apparatus was employed for the dielectric constant measurements. Pressures were measured with an oil-operated deadweight gauge. The isobutane sample was separated from the oil by a diaphragm-type differential pressure indicator. The primary temperature sensor was a platinum resistance thermometer.

For the magnetic suspension densimeter used in the present work, the magnetic moment of the float material is a relatively strong function of temperature. Thus, it is most practical to take data along isotherms. For each temperature, the cell was first filled to the highest pressure (35 MPa) for that run. Data points at lower pressures were taken after venting appropriate amounts of gas. For each isotherm the last point was taken on the coexistence boundary to compare with previous saturated-liquid density results (*6*) obtained with a magnetic suspension densimeter in this laboratory. The present saturated-liquid data agreed with those taken earlier to better than 0.02% and are not published here since they were used only as a check on the present work. (Saturated-liquid dielectric constants obtained in the present study have been published elsewhere (*5*).) Vacuum measurements, needed at each temperature for absolute density measurements with the magnetic suspension densimeter used here, were obtained, for each run, before charging the cell with liquid isobutane.

The samples were obtained from cylinders of research-grade, commercially available liquid isobutane. The minimum purity as specified by the supplier was 99.90 mol %, with the most probable impurity being *n*-butane.

Results and Discussion

The experimental densities (ρ) and dielectric constants (ϵ) for liquid isobutane are given as a function of temperature (T, IPTS-68) and pressure (P) in Table I. Also presented in this table are values for the Clausius–Mossotti function (CM) calculated from the relation

$$\mathrm{CM} = \left(\frac{\epsilon - 1}{\epsilon + 2}\right)\frac{1}{\rho} \qquad (1)$$

Data have been obtained for 11 isotherms between 120 and 300 K. Two of the isotherms (at 140 and 160 K) were repeated on new samples to determine the reproducibility of the measurements. Each isotherm was comprised of 12 data points taken at pressures approximately equal to those for any other isotherm. The density range for this work extended from 551 kg/m^3, or approximately 2.5 times the critical density, to 749 kg/m^3, which is slightly greater than the triple-point density.

The estimated total uncertainty in the experimental densities is less than 0.1% while the imprecision of the measurements is a few parts in 10^4 (*3*). The estimate of the imprecision was substantiated by the reproducibility of the isotherms at 140 and 160 K on different liquid samples. Capacitance measurements to a resolution of 10^{-4} pF, combined with better than 10^{-4}-pF stability in the vacuum capacitance, gave an estimated uncertainty of approximately 0.01% in the dielectric constant. For pressure, the overall uncertainty was approximately 0.01%, increasing somewhat at lower pressures. Temperatures were measured to a precision of a few mK; however, the total uncertainty could be as large as 30 mK at 300 K, decreasing to approximately 15 mK at 120 K.

The density and dielectric constant data from this work have been used in comprehensive correlations (*7*, *8*) of the thermophysical properties of isobutane. Only one other set of data